Keep it Flat

The Influence of Backside Particle Contamination on Wafer Deformation during Chucking

Twan Bearda, Frank Holsteyns, Karine Kenis, Paul Mertens – IMEC
Aschwin van Meer – ASML Holding NV
Don Brayton, Lisa Cheung – KLA-Tencor Corporation

Backside particle contamination can cause deformations of the substrate during chucking. These defects, commonly called 'hot spots,' typically occur during lithographic exposures or CMP. Previous analysis has shown that the maximum wafer deflection is strongly reduced by plastic deformation of the particles. This article presents a promising study in which particles of different materials such as silica, silicon, tungsten and polystyrene latex (PSL), different sizes, and different densities are deposited on the backsides of 300mm wafers. The resulting changes in flatness during chucking are measured, and found to agree well with theoretical predictions.

The presence of contamination at the backside of a wafer can compromise the yield of advanced semiconductor devices via several mechanisms:

- Transport (through air or through liquids) from the backside of a wafer to the front of an adjacent wafer
- Degraded contact with electrostatic or thermal chucks, resulting in arcing or temperature non-uniformities
- Flatness changes during chucking (hot-spots), affecting processes such as lithography (loss of DOF budget) and CMP (non-uniform polishing rate)

This study focuses on flatness changes due to backside particles. The 2005 edition of the ITRS Roadmap presents stringent requirements concerning backside contamination[1], but minimal quantitative data have been published on this topic. While no specifications are given in Table 67 of the ITRS roadmap (Front End Preparation), the footnotes suggest a critical particle size of 230nm for the year 2006. The model used to support this assumes 40% compression of a particle during chucking, and a DOF budget loss that equals 2CD. Table 77 (Lithography) suggests a critical particle size of 120nm.

It was recently proposed[2] that plastic deformation of the particle significantly reduces DOF budget loss. A model was developed that predicts a dependence on particle size and material. This article presents experimental data that support the model. The flatness change of wafers is measured after contaminating wafer backsides with different particle types and sizes. The data show that, in the case of particle clustering, the total volume of the particles determines the flatness change of the wafer.

Experimental Set-up

In the experimental procedure (figure 1) the flatness of two pairs of 300mm wafers is measured on the leveling system of an ASML TWINSCAN™. The scanner contains two identical chucks that are not flat, but covered by pins or 'burls' (figure 2). The diameter and position of these pins is designed to minimize the contact area with the wafer (approx. 3%) while maintaining good wafer flatness. The pins are made of a hard material and have a surface roughness that is negligible compared to the particle sizes relevant in this experiment. Prior to the flatness measurement, ten clean dummy wafers are cycled on each chuck to remove accidental residual contamination. The particle deposition – in different areas on the backside of one wafer of each wafer pair – is carried out by forming an aerosol from a particle-containing aqueous solution.

For each deposition spot, the particle material, particle size, particle density, and deposition spot diameter are varied. It is difficult to control the size and density of the deposited particles because of the deposition method, the limited availability of the particles in the requested size range, and the stability of the aqueous solution. The actual values are easily determined, however, using a KLA-Tencor Surfscan™ SP1 unpatterned surface inspection tool equipped with a Backside Inspection Module (SP1-BSIM).

After particle deposition, the flatness of the two wafer pairs is measured again using the same procedure as before, with each wafer measured on the same chuck as in the first measurement. The uncontaminated wafer of each pair is measured before the contaminated one. Assuming that the intrinsic wafer flatness

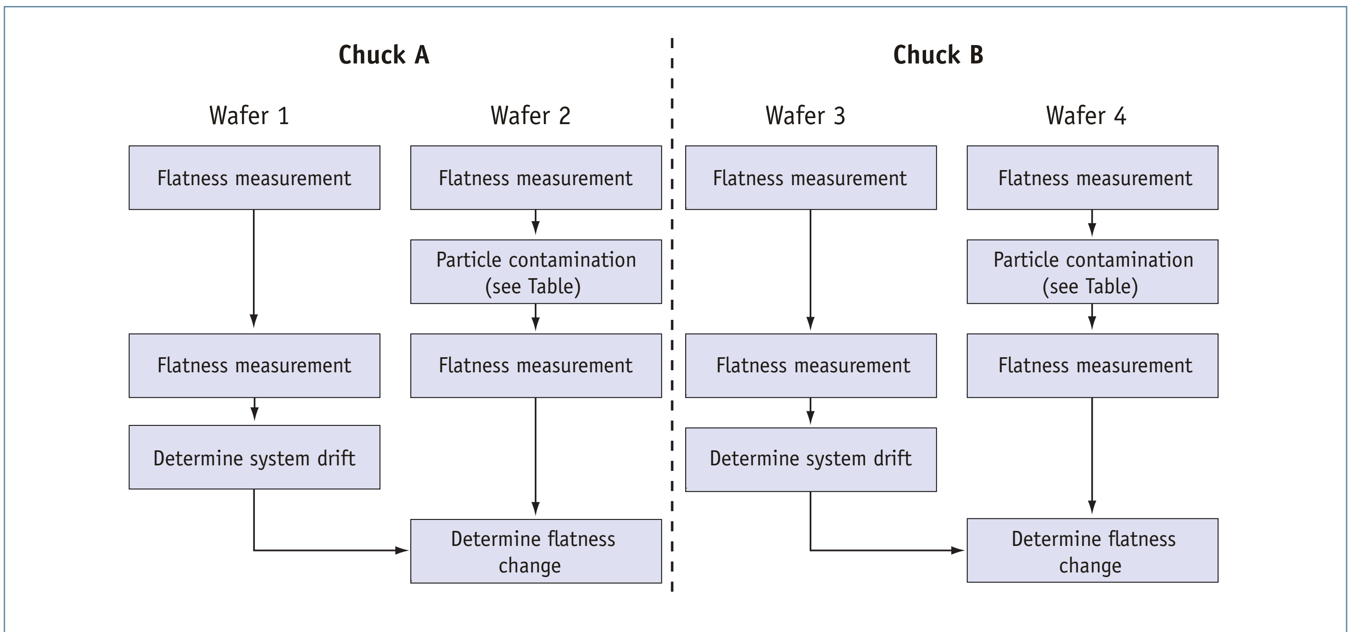

Figure 1: Experimental flow.

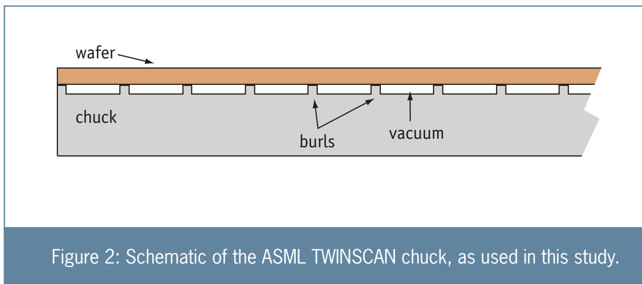

Figure 2: Schematic of the ASML TWINSCAN chuck, as used in this study.

does not change significantly during the experiment, it is possible to use this sequence to correct for the drift of the leveling system and for the intrinsic flatness of the contaminated wafers. The resulting flatness change is considered to be solely due to the backside particle contamination.

Note that the two pairs of wafers are shielded by two "umbrella wafers" to minimize uncontrolled particle contamination during all transport. At each step, measurements using the SP1 or SP2 tools help to verify that no uncontrolled contamination occurs during the procedure. Also, before and after the flatness measurement, a KLA-Tencor 23xx bright-field inspection tool is used for extensive review of the deposited particles.

Figure 3 shows the light-scatter maps for the backsides of wafers 2 and 4 after particle deposition. The maps are mirrored to show the actual particle positions when the wafer backside faces down. The particle size histograms for each deposition spot are shown in figure 5 for wafer 2. Additional data are also available for wafer 4 (for comprehensive experimental data, tables and figures, please refer to the original poster presented by the authors at SPIE 2006[4]). Moreover, for reasons that will become clear later, the figures also show the integrated particle volume as a function of particle size. The radii of the deposition spots are listed in table 1.

Figure 4 graphically represents the flatness changes of wafers 2 and 4. Different deflection areas corresponding to different deposition spots are clearly discerned. The detection limit for flatness changes is typically 25nm, however, the interpretation of the results only considers flatness changes larger than 50nm. Table 1 also shows the maximum deflection for each deposition spot, determining the area of the regions (DL) where the flatness change exceeds 50nm. The equivalent radii of these areas are also listed.

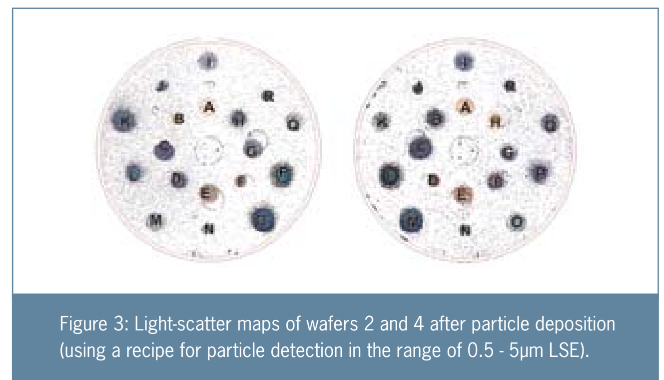

Figure 3: Light-scatter maps of wafers 2 and 4 after particle deposition (using a recipe for particle detection in the range of 0.5 - 5µm LSE).

Theoretical Considerations

A previous report[2] considered the deflection of a wafer due to a point force. In this model, the impact of burls is considered negligible, so the chuck is modeled as a flat surface. The wafer deflection w(r) has a maximum at r=0 and extends over an area with radius a. At r=a, the wafer is no longer deformed (figure 6):

$$w(r) = -\frac{qa^4}{64D}\left(1 - \frac{r^2}{a^2}\right)^2 \qquad (1)$$

Deposition spot	Wafer 2			Wafer 4		
	Deposition radius (mm)	Spot deflection radius (mm)	Area maximum deflection (nm)	Deposition radius (mm)	Spot deflection radius (mm)	Area maximum deflection (nm)
A	12.5		DL	12.5		DL
B	6.25		DL	6.5		DL
C	12.5	12.3	302	12.5		DL
D	8	10	689	9		DL
E	12.5		DL	12.5	11.5	1360
F	7		DL	7.5		DL
G	12.5	7.3	154	14		DL
H	8.5	12.3	1386	10	14.9	1548
I	12.5	6	146	12.5	10.8	960
J	6.25	5.5	161	6.25	5.5	110
K	13.5	17	1729	12.5	4.8	69
L	8	10.7	1051	10	8.4	438
M	12.5	4.9	100	10.5	10	999
N	6.5	2.9	60	6.5	3.4	91
O	14	17.4	1766	15	3	66
P	9.5	13.8	2314	12.5	14	810

Table 1: Radii of deposition spots, and the characteristics of the corresponding deflection areas.

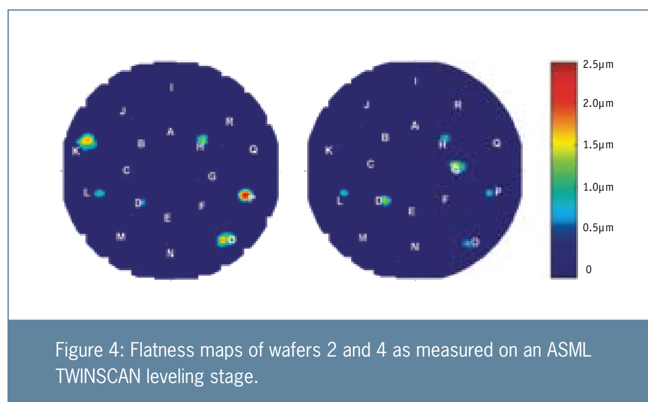

Figure 4: Flatness maps of wafers 2 and 4 as measured on an ASML TWINSCAN leveling stage.

The constant D is the flexural rigidity, which is determined by material properties and the thickness of the wafer. For standard 300mm wafers, D=5.5nm. In many cases, it is found that the force required for deflection exceeds the material strength of the particle. Therefore, plastic particle deformation occurs in order to reduce the deflection and to increase the contact area between wafer and particle. Assuming a cylindrical shape for the particle, it is possible to estimate the resulting deflection as a function of particle size.

Experience shows that backside particles often occur in clusters. In this experiment too, a large number of particles are present within each deflection area. Therefore, a discussion of particle clusters is desirable. The case of two particles that are located close to each other compared to the radius a of the deflection area is discussed. This means that the deflection can still be considered as being caused by a point force. The particles have a cylindrical geometry as before and different sizes (see table 2 and figure 7).

The discussion assumes that the initial height $s_1 > s_2$. Initially, maximum deflection $w_{max} = s_1$ and no plastic deformation occurs. Then, particle 1 is deformed to reduce its height; the particle/substrate contact area is then given by V_1/w_{max}. This process continues until $w_{max} = s_2$. From this moment, the smaller particle also contacts the substrate, and the contact area increases from V_1 / w_{max} to $(V_1 + V_2) / w_{max}$. This argument helps deduce that in case of particle clusters, the total particle volume determines the wafer deflection.

Discussion of Results

The results clearly show a dependence of the wafer deflection on the particle material and particle density. In the case of tungsten or silicon particles, a deflection is always observed. PSL or silica spheres only cause a wafer deflection if the size of the deposited particles is large enough. This is expected because of the softness of the PSL and the brittleness of the silica (the chemically grown silica spheres are very porous). However, another explanation for the small wafer deflections is presented below.

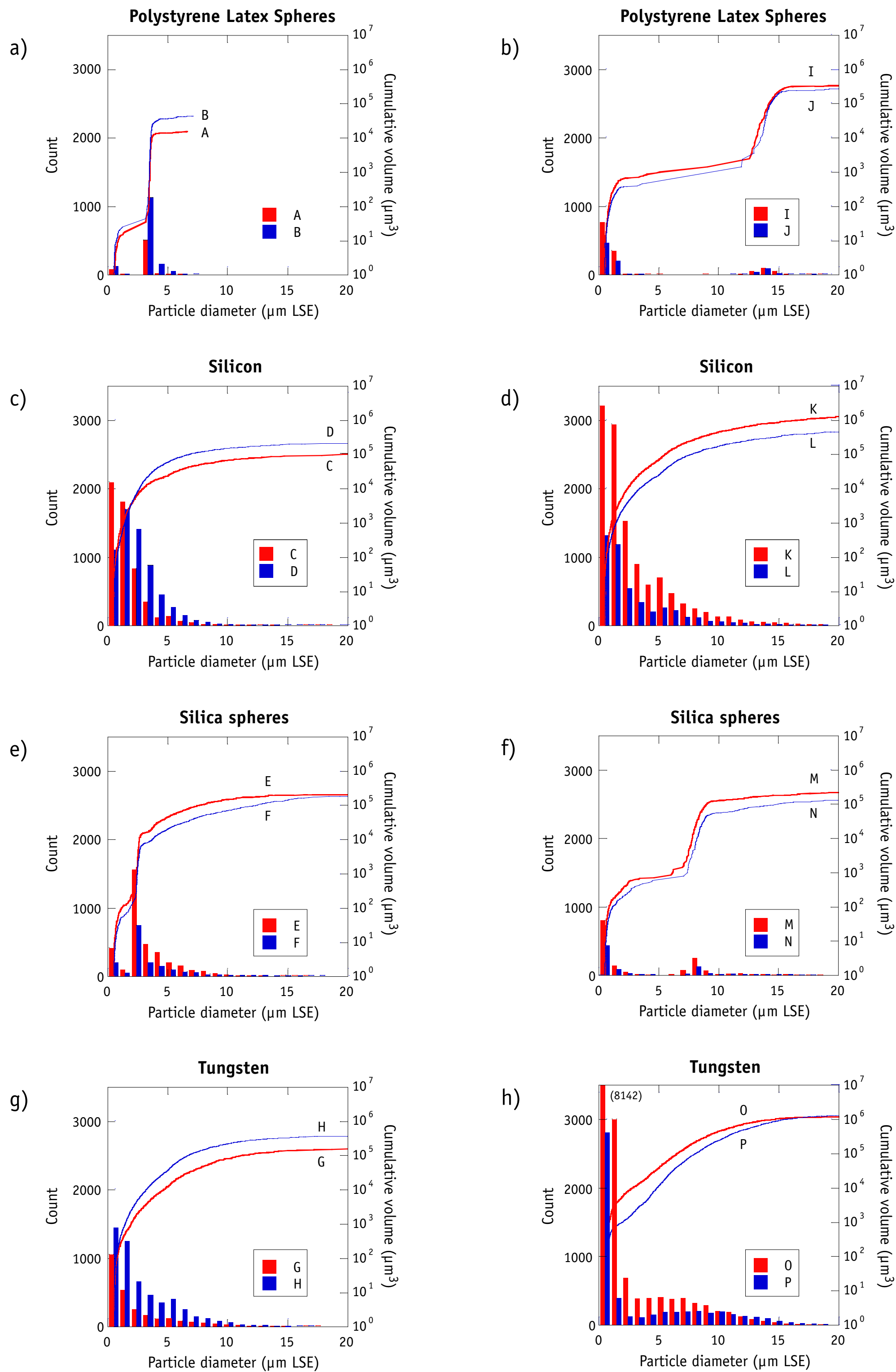

Figure 5: Particle size distributions on wafer 2. Bars show the size histogram (bin size: 1µm), and lines represent the cumulative particle volume.

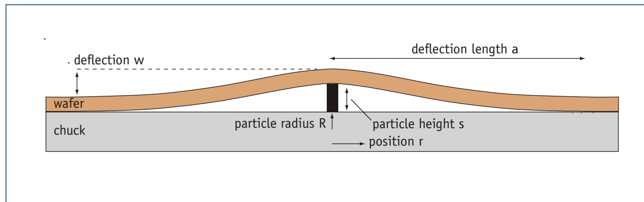

Figure 6: Schematic of the model for wafer deflections induced by backside particles.

	Particle 1	Particle 2
Initial height	$s_1 = (4/\pi\ V_1)^{1/3}$	$s_2 = (4/\pi\ V_2)^{1/3}$
Initial radius	$R_1 = \frac{1}{2}\ s_1$	$R_2 = \frac{1}{2}\ s_2$
Volume	V_1	V_2

Table 2: Dimensions of a cluster of two particles.

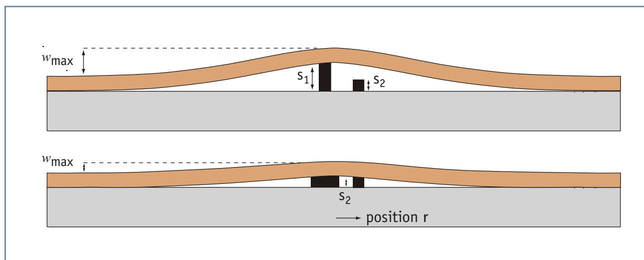

Figure 7: Wafer deformations of two particles, where (top) only the largest particle is deformed and (bottom) both are deformed.

The model presented previously relates the maximum wafer deflection to the radius of the deflection area (Equation 1 with r=0). Figure 8 shows this relation along with the experimental data obtained in this experiment. Although the experimental data follow a trend that is very similar to the theoretical curve, most data points are located at the right of the curve. This is because the curve is derived under the assumption of a point force. In contrast, the particles are distributed over a large area in this experiment, thus artificially broadening the deflection area.

This discussion on clustered particles helps conclude that, for the analysis of the effect on wafer deflection, the total particle volume should be taken into account. This parameter is shown as drawn lines in figure 5 for wafer 2 (for complete wafer 4 data, refer to SPIE poster[4]) . Clearly, although small particles are much more abundant than large particles, their effect on total particle volume is limited in our experiment. Also, the total particle volume is relatively stable at large particle sizes, so the experimental error can be considered small.

Since only 3% of the wafer is in contact with the chuck of the ASML TWINSCAN, it is expected that only 3% of the particles have an impact on the wafer flatness change. Ideally, these particles are identified by comparison of the coordinates of the chuck pins and the light-scattering results. However, both the placement of the wafer on the chuck, and the particle coordinates obtained from the defect reviews are not accurate enough for such an analysis. Therefore, the volume of the particles that have an impact on the wafer flatness is assumed to be 3% of the total particle volume shown in figure 5.

The particle sizes in the figures are Latex Sphere Equivalent (LSE), i.e. they represent the sizes of PSL spheres that would have the same scattering efficiency as the actual particles. Because the scattering efficiency depends on the material that the particle is made of, the LSE size is different from the actual size. For particles larger than the SP1 wavelength (488nm), Mie scattering occurs. The intensity of the reflected light is

$$\frac{I_{s,\,Mie}}{I_0} = \pi R^2 \cdot Q_s \qquad (2)$$

where I_0 is the intensity of the incoming light, R the radius of the particle, and Q_s the scattering efficiency. The product $C_s = \pi R^2 \cdot Q$ is called the scattering cross-section of the particle. Q_s is obtained by numerical calculations[3], and is shown in table 3 for the materials of interest in this study. Also shown is the correction factor applied to PSL-equivalent particle radii obtained from SP1 measurements.

Figure 9 shows the results of the deflection analysis for wafer 2 (results for wafer 4 in original SPIE poster[4]). The drawn line is the theoretical prediction assuming yield strength of 1 GPa. The dashed line indicates the limit where the wafer deflection equals twice the particle radius (single-particle case). This shows wafer deflection as a function of particle radius (volume). For particle clusters, the particle radius is only an 'effective radius' representative of the cumulative volume of the cluster. The results from the complete data are very similar, indicating that the experiment is well controlled and reproducible. Comparing the different particle materials, it appears that the small deflections in the case of PSL and silica particles are mainly due to the small particle volume. Apparently the differences in particle yield strength are too small to be observed on a log scale in this experiment. In general, experimental data are of the same order of magnitude as the theoretical predictions, and they follow a similar trend.

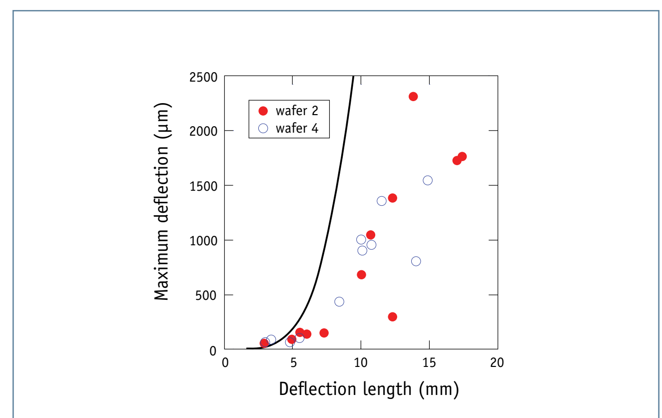

Figure 8: Maximum wafer deflection as a function of deflection length.

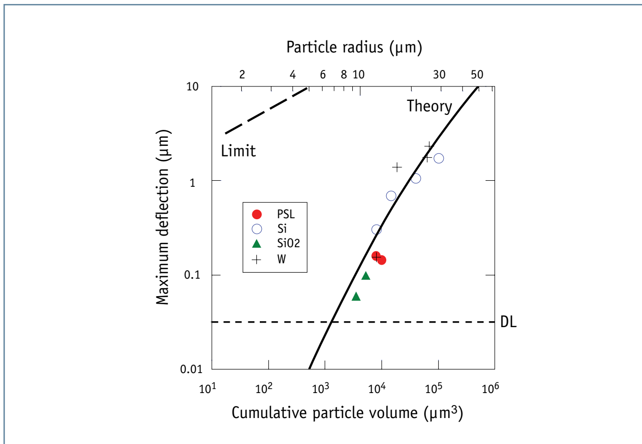

Figure 9: Wafer deflections of wafer 2 as a function of cumulative particle volume or particle radius. PSL equivalent radii and volumes have been scaled as discussed in the text.

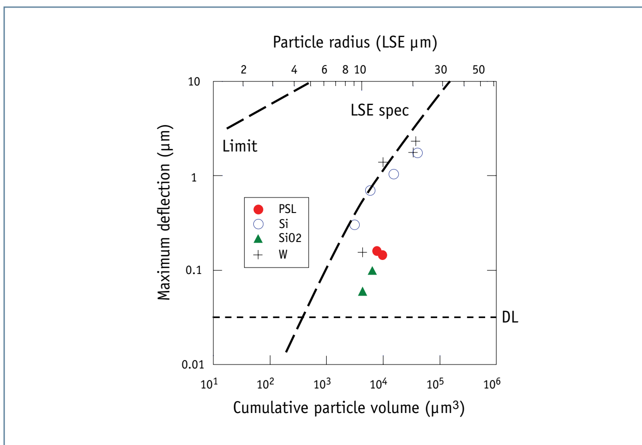

Figure 10: Wafer deflections of wafer 2 using LSE particle dimensions.

Figure 10 shows the same results for wafer 2 as figure 9, but without applying the correction for differences in scattering efficiency (table 3). The line labeled "LSE spec" is a deflection limit based on the theoretical prediction, taking into account that LSE particle diameters may be 30% smaller than actual particle diameters. Clearly, without correction the wafer deformation would have been greater than anticipated, and the particle material dependence might have been wrongly attributed to different yield strengths. More importantly, during inspection the particle material is generally not known, and the particle diameter is expressed in μm as LSE. Critical particle diameters should be converted to this unit, which yields values that may typically be 30% smaller than the values for actual particle diameters.

A random review on defects before and after chucking indicates that most of the particles are not impacted because a chuck pin does not make contact with them. In at least one case, however, the particle is clearly crushed during the chucking. Figure 11 shows the same result in a larger area along with another particle (not crushed) in the same deposition spot.

	Refractive index (λ=488nm)		Mie scattering	
Material	**n**	**k**	**Q_S**	**R_{actual} / R_{PSL}**
PSL	1.61	0	2.04	1.00
Silicon	4.42	0.02	1.44	1.19
Tungsten	2.47	1.92	1.45	1.19
Silica	1.46	0	2.20	0.96

Table 3: Sizing of particles relative to PSL particles.

Conclusions

This study investigates wafer deflections due to backside particles during chucking. The experimental data show that the deflections depend on the material, size and density of the particles. The results are explained by plastic deformation of the particles. Low particle densities and small particle sizes are found to cause a smaller wafer deflection. In the case of particle clusters, the total particle volume determines the wafer deflection. As a rule of thumb, one may assume a critical particle volume of 1000μm³ LSE for a wafer deflection of approximately 100nm.

References

1. International Technology Roadmap for Semiconductors, Edition 2006. http://public.itrs.net, January 2006.
2. T. Bearda, Effect of Backside Particles on Substrate Topography, Japanese Journal of Applied Physics 44 (2005) 7409-7413.
3. Software used: P. Laven, MiePlot v3.4.16, October 2005. http://www.philiplaven.com, December 2006.
4. Original poster presented at SPIE 2006, Twan Bearda, Frank Holsteyns, Karine Kenis, Paul Mertens, Aschwin van Meer, Don Brayton, Lisa Cheung, "The influence of backside particle contamination on wafer deformation during chucking", in Metrology, Inspection, and Process Control for Microlithography XX.

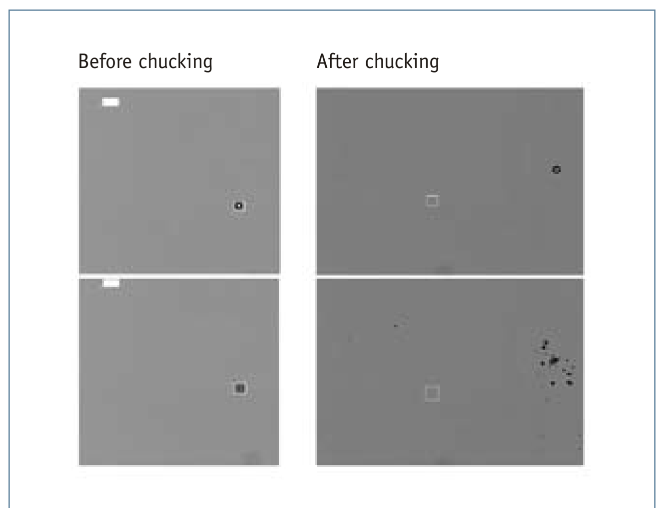

Figure 11: Backside particles, located in deposition spot M2, before and after chucking. One of the particles is crushed during chucking.